# Spectroscopic Investigations of Polyamido Amine Starburst Dendrimers Using the Solvatochromic Probe Phenol Blue

**Dana L. Richter-Egger, Jeff C. Landry, Aaron Tesfai, and Sheryl A. Tucker***

*Department of Chemistry, University of Missouri~Columbia, Columbia, Missouri 65211-7600*

*Received: January 4, 2001; In Final Form: March 30, 2001*

The physical and chemical properties of PAMAM-AT dendrimers' interior were investigated using the fluorescent, solvatochromic probe phenol blue. In aqueous solutions of each generation studied except G0, two discrete dye populations were clearly observed. PAMAM-AT dendrimers were shown to form a tight, nonpolar association with the majority of available dye within the dendrimer interior, probably near its core. In the absorption and steady-state fluorescence emission spectra, a microenvironment of decreasing polarity in increasingly larger-generation PAMAM-AT dendrimers (up to G3) is seen for the associated probe. The remaining larger-generation dendrimers (G4−8) all provide a microenvironment of essentially equal polarity. Fluorescence anisotropy values for phenol blue in the PAMAM-AT dendrimers demonstrate the dye's sensitivity to the changing molecular volumes of the dendrimer generations. Model compounds that mimic PAMAM-AT's surface groups and branching moieties were used to better define the associated dye's location. The mimics further confirm that phenol blue is associated inside the dendrimer, where it does not interact with the dendrimer surface groups.

## Introduction

Dendrimers are a unique, highly diverse class of polymers that, unlike traditional polymers, have well-defined macromolecular architecture. They are constructed from a core unit by stepwise attachment of branching unit layers, called generations (G). This is described pictorially for amine-terminated polyamidoamine (PAMAM-AT) dendrimers in Figure 1. Dendrimers are described as unimolecular micelles[1−4] due to their similar structural features. Carboxylate-terminated polyamidoamine dendrimers (PAMAM-CT) are analogous to anionic micelles, and PAMAM-AT dendrimers are analogous to nonionic or cationic micelles, depending on the pH. Micelles form only at concentrations above the critical micelle concentration, vary significantly in size and shape, and are dynamic systems in which free surfactant monomers continuously migrate in to and out of the micelle. Dendrimers, however, do not share these properties. Instead, they are monodisperse,[5] covalently bound molecules at all concentrations, stable over a large pH range,[6] and easily functionalized.[7,8] Their solubility and stability can be synthetically tailored for use in many organic solvents. Therefore, the substitution of dendrimers into current micellar applications may be particularly useful. Suggested dendrimer applications are as diverse as their structures. For example, they have been used as gene transfer agents,[9−12] a promising AIDS vaccine,[13] catalysts,[14−17] radiotheraputic agents,[18] and substitutes for micelles in micellar electrokinetic chromatography.[8,19−23]

PAMAM dendrimers have received considerable attention because they are commercially available in many different sizes/generations. PAMAM-CT dendrimers, particularly their surfaces, have been characterized by spectroscopic methods.[24−37] However, significantly less information is published about the PAMAM-AT dendrimers, in part because they have been more challenging to study. In fact, to our knowledge, very little spectroscopic evidence has been published concerning the interior of PAMAM dendrimers, irrespective of the surface groups. An improved understanding of the chemical and physical properties of the interior regions of PAMAM-AT dendrimers is vital to their successful use in future applications.

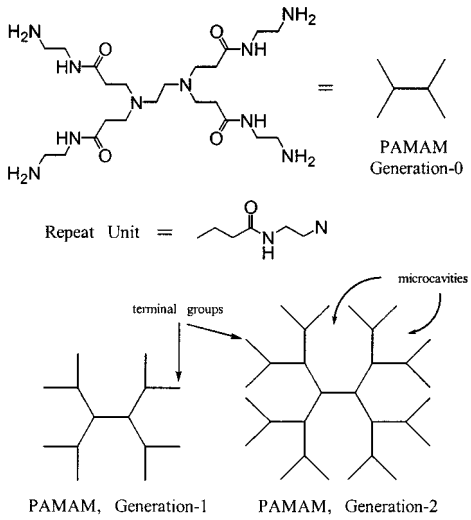


**Figure 1.** Architecture of a PAMAM Dendrimer (Modeled after Chart 1 in Pistolis[28]).

The purpose of this work is to advance the knowledge of those novel microenvironments contained within the PAMAM-AT dendrimers, specifically their accessibility, polarity, relative size, and generational dependence. Our approach is to use a solvatochromic probe molecule that associates within the interior of PAMAM-AT dendrimers. Difficulties reported in previous spectroscopic probe studies of PAMAM-AT dendrimers include fluorescence quenching by the tertiary amine groups,[28] com-

* To whom correspondence should be addressed. E-mail: TuckerS@missouri.edu.

10.1021/jp0100396 CCC: $20.00 
Published on Web 06/19/2001

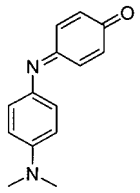

**Figure 2.** Chemical structure of phenol blue.

plete failure to associate,[31] and interference by a fluorescent background signal,[28,38] attributed to the PAMAM dendrimers.

A recent study of PAMAM-AT dendrimers with the well-known fluorescent, solvent polarity probe pyrene reported enhanced solubility and increased protection of pyrene from aqueous solution. However, this study only included the smallest generations, G0−2,[28] which have little to no tertiary structure[39] compared to larger generations. Our previous studies[40] using Reichardt's dye (ET-30), a well-known absorption, solvent polarity probe, primarily addressed the near-surface polarity and surface accessibility for a large number of PAMAM-AT generations (G0−8) and indicated a microenvironmental polarity similar to 1-decanol. Though we concluded that ET-30 penetrated beyond the surface of the dendrimer, it was clear that this relatively large molecule was not completely encapsulated by the dendrimer. We also concluded that additional studies with a smaller probe molecule would provide a more complete picture of the interior cavities of PAMAM dendrimers.

In this current study, information about PAMAM-AT dendrimers' interior is acquired from the association of a significantly smaller spectroscopic probe—phenol blue (Figure 2). The generational dependence of these properties is also closely examined. Like ET-30, phenol blue has a solvatochromic absorption band in the visible region, away from the dendrimers' absorption/fluorescence. Unlike ET-30, phenol blue also has a solvatochromic fluorescence emission band, and it is significantly smaller in size. In contrast to previous fluorescent probe studies,[25,28] the fluorescence emission of phenol blue is not quenched by PAMAM-AT's tertiary amine groups. Our data suggests that it associates within the dendrimer, well beyond the surface.

The retention of phenol blue's fluorescence emission in the presence of the PAMAM-AT dendrimers allows for a more detailed characterization of the physical properties of their interior. Spectrofluorometric probe techniques provide realistic views of macromolecular media in fluid solution.[41−43] They are especially powerful when used in combination and enable one to develop a more complete and accurate picture.[44] Important advantages of fluorescence spectroscopy include minimal sample perturbation, high sensitivity, and subnanomolar detection limits.[45,46]

The physical[47−49] and spectroscopic absorption properties[50−53] of phenol blue have been well characterized, and the dye is believed to exist solely as the neutral quinoneimine[47] in both protic and aprotic solvents of varying polarities. The dye's solvatochromic absorption band shifts to shorter wavelengths as the solvent polarity decreases and has a $\lambda_{max}$ range from 660 nm in trifluoroethanol to 550 nm in *n*-heptane.[50] To our knowledge, phenol blue has not been used to study organized media, but its structural analogue, nile red, which is also a solvatochromic probe, has been used extensively to study proteins, lipids, enzymes, and PAMAM dendrimers with modified cores.[54−58] Another structural analogue of phenol blue, cationic methylene blue has been used to study the anionic surfaces of PAMAM-CT dendrimers.[32,35] Mimics of PAMAM-AT's surface and branching moieties are also examined to help determine the associated dye location.

## Experimental Section

**Materials.** Amine-terminated PAMAM dendrimers with tetrafunctional ethylenediamine (EDA) cores were obtained in methanol from Dendritech (Midland, MI) and stored at 0 °C. Other materials were obtained from the following suppliers: *N*-ethylacetamide (*N*-EAA), phenol blue, triethylamine, and propylamine (Aldrich); 200 proof ethanol (McCormick); and HPLC grade water, toluene, acetone, acetonitrile, *N*,*N*-dimethylformamide (DMF), dichloromethane, tetrahydrofuran (THF), and methanol (Fisher). All chemicals were used as received.

*Sample Preparation.* Stock solutions of phenol blue were prepared by dissolving the dye in tetrahydrofuran (THF) and were stored in the dark at room temperature. Samples were prepared by quantitatively transferring known aliquots of the phenol blue stock solution into volumetric flasks where the solvent was stripped off under ultrahigh purity nitrogen. Appropriate volumes of PAMAM-AT dendrimers in methanol were quantitatively transferred to the flasks where the solvent was also stripped off under nitrogen. It may not be possible to completely remove all of the methanol from the larger generations; however, trace amounts of methanol do not appear to affect the dendrimers structure[59] or our experimental results. The samples were diluted to volume with organic solvent or HPLC grade water − [phenol blue] = $1 \times 10^{-6}$ M and [dendrimer] = $1 \times 10^{-4}$ M. These samples were stirred for ∼24 h to facilitate dye and dendrimer solubilization, followed by an additional ∼24 h equilibration in the dark at room temperature.

**Methods.** *UV/Vis Absorption Measurements.* Absorption spectra were collected in 1 $cm^2$ Suprasil quartz cuvettes on a Hitachi U-3000 (Hitachi Instruments, Danbury, CT) double-beam spectrophotometer with a scan rate of 120 nm/min, a slit width of 1 nm, and a thermostated cell temperature of 25 °C. Spectra were blank corrected for the possible absorption of solvent and the aqueous dendrimers, though no background signal due to the dendrimers was apparent in the wavelength region of interest.

*Steady-State Fluorescence Measurements.* The fluorescence emission spectra and steady-state anisotropy data were collected in 1 $cm^2$ Suprasil quartz cuvettes on a SLM 48000 DSCF/MHF spectrofluorometer (Jobin Yvon, Edison, NJ) at a temperature of 25 °C. The excitation source was an Ion Laser Technology (Salt Lake City, UT) RPC-50-220 argon ion laser operated at 514 nm and 30 mW.

For fluorescence emission spectra, the emission monochromator slit widths (entrance and exit) were set at 16 and 4 nm, respectively. The emission scan interval was 1 nm, and measurements were recorded from an internal average of three signal samplings per emission wavelength. The fluorescence emission was passed through a polarizer set at 0° to correct for the Woods anomaly.[60] Spectra were also absorption and solvent blank corrected.

Steady-state anisotropy measurements were collected in "L" format[61] using a 550 nm long-pass filter (KV550 Schott Glass Technologies, Duryea, PA) and a 600 nm short-pass filter (03 SWP 610 Melles Griot, Irvine, CA). The means and standard deviations were calculated from five sample replicates, each containing an internal average of five signal samplings at each of the four polarizer orientations (0°−0°, 0°−90°, 90°−0°, 90°−90°).

**TABLE 1: Solvent Polarity Wavelength Dependence of Phenol Blue**

| solvent | experimental absorption $\lambda_{max}$ (nm)[a] | literature[b] absorption $\lambda_{max}$ (nm) | fluorescence emission $\lambda_{max}$ (nm)[a,c] |
|---|---|---|---|
| 2,2,2-trifluoroethanol | 660 | 660 | *e* |
| water | 652 | *d* | *e* |
| methanol | 608 | 608 | 620 |
| dimethylformamide | 593 | 595 | 618 |
| *N*-ethylacetamide | 584 | *d* | 618 |
| acetone | 581 | 582 | 602 |
| toluene | 569 | *d* | *e* |
| *n*-heptane | 541 | 550 | *e* |

[a] $T = 25$ °C. [b] Taken from Kolling.[50] [c] Fluorescence $\lambda_{ex} = 514$ nm. [d] No value reported. [e] No fluorescence observed.

*Fluorescence Lifetime Measurements.* Fluorescence lifetimes were collected in the frequency domain[62,63] on the same SLM 48000 DSCF/MHF spectrofluorometer, which also has multiharmonic, Fourier transform phase-modulation capabilities. The excitation source was a Coherent (Santa Clara, CA) Innova 307C argon ion laser operating at 514 nm and 500 mW. In the MHF mode, however, only a small fraction of the excitation power is actually used to interrogate the sample. A base frequency of 4.0 MHz and a cross-correlation frequency of 7.000 Hz were used in all dynamic measurements. Ten pairs of sample/reference measurements were collected in triplicate for each sample, and each measurement contained 100 internal averages. An aqueous scatter solution of kaolin (Sigma) was used as the lifetime reference. The same 550 lp/600 sp filter combination used for anisotropy measurements was also used for the lifetime measurements.

The lifetimes and fractional intensities were obtained from the phase and modulation data using the maximum entropy method (MEM).[64−66] Advantages of using MEM compared to traditional nonlinear least squares (NLLS) are documented and include the fact that MEM is self-modeling, does not require selection of an a priori model, and returns more consistent lifetime distributions.[43,45,65−68] The three replicate phase and modulation data sets collected for each sample were analyzed both individually and as a combined file. The lifetime window consisted of 500 discrete, equally spaced cells from 0.01 to 10 ns.

## Results

**Solvatochromic Behavior of Phenol Blue.** Because of variations in instrumental and experimental conditions from laboratory to laboratory,[69−71] an in-house "solvent polarity ruler" for phenol blue was generated. Solutions of phenol blue were prepared in several neat solvents, and their absorption and emission spectra recorded. Experimentally obtained absorption and fluorescence $\lambda_{max}$ values, as well as absorption $\lambda_{max}$ values published in the literature,[50] are shown in Table 1. Differences are within acceptable experimental error, particularly in light of the fact that these absorption bands are broad, up to ~200 nm in several solvents studied. These solvent polarity experiments also indicated that the dye's fluorescence quantum yield markedly decreases, and eventually the signal becomes virtually absent at the two solvent polarity extremes. It is also important to note that though the PAMAM-AT dendrimers are slightly basic (measured pH = 8−10), the observed $\lambda_{max}$ shifts are not due to a pH response by phenol blue. The dye showed only a very small blue shift (5 nm) in its solvatochromic absorption band within this pH range.

**UV/Vis Absorption Spectroscopy.** Representative absorption spectra of phenol blue in water and aqueous PAMAM-AT dendrimers are shown in Figure 3. All spectra, with the exception of the water spectrum, clearly show varying contributions from the same two absorption bands centered at 560 and 646 nm. The band at 560 nm is due to a rather nonpolar microenvironment, and the band at 646 nm is indicative of a much more polar microenvironment, believed to be predominantly aqueous. As the generations of PAMAM-AT increase, the band indicative of a relatively nonpolar microenvironment consistently increases in intensity at the expense of the band due to the predominantly aqueous microenvironment. For the smallest generation dendrimers (G0−1), a band at 646 nm is predominant and is quite similar to the spectrum observed for phenol blue in water. The intensity of the 560 nm band systematically increases for G2−4 and is relatively constant for G4−7. The largest PAMAM-AT generation studied, G8, does not follow this trend. Compared to G7, it shows a decreased absorbance of the 560 nm band and increased absorbance of the 646 nm band.

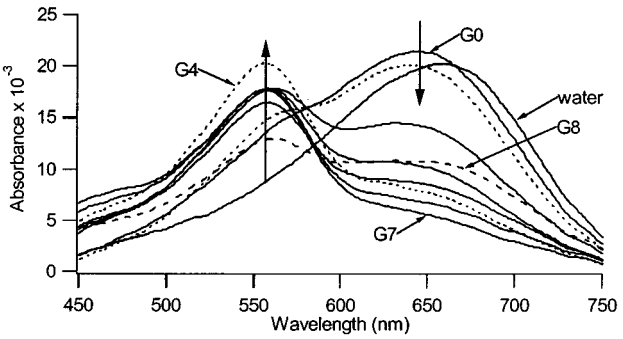


**Figure 3.** Representative absorption spectra of phenol blue [$1 \times 10^{-6}$ M] in aqueous PAMAM-AT dendrimers [$1 \times 10^{-4}$ M]. Experimental conditions: $T = 25$ °C.

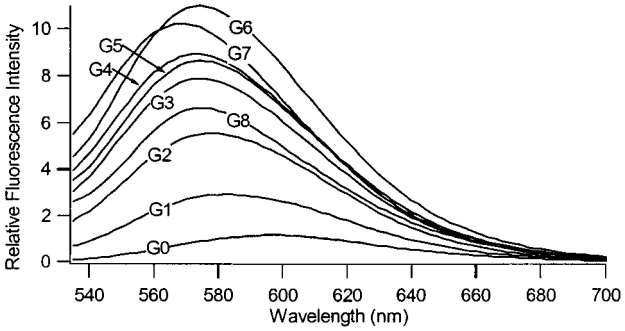


**Figure 4.** Representative steady-state fluorescence emission spectra of phenol blue [$1 \times 10^{-6}$ M] in PAMAM-AT dendrimers [$1 \times 10^{-4}$ M], absorption- and blank-corrected. Experimental conditions: $\lambda_{ex} = 514$ nm and $T = 25$ °C.

**Steady-State Fluorescence Emission Spectroscopy.** Representative fluorescence spectra, corrected for the solvent and differential absorption at the excitation wavelength, are shown in Figure 4. Phenol blue in the presence of aqueous PAMAM-AT dendrimers has a single, broad solvatochromic fluorescence emission band. There is a gradual blue shift of this band for G0−2, indicating decreased microenvironmental polarity. There is also a pronounced increase in the relative fluorescence intensity as the dendrimer generations become progressively larger, up to G3. Fluorescence spectra of phenol blue in the larger-generation dendrimers (G3−7) are all relatively similar in both the $\lambda_{max}$ (572 nm) and relative intensity, with the exception of G8. The magnitude of the emission intensity increase for G6 and 7 is less than that seen for the smaller generations. In addition, the largest spectral blue shift occurs for G7. Generation 8 has decreased emission intensity, analogous

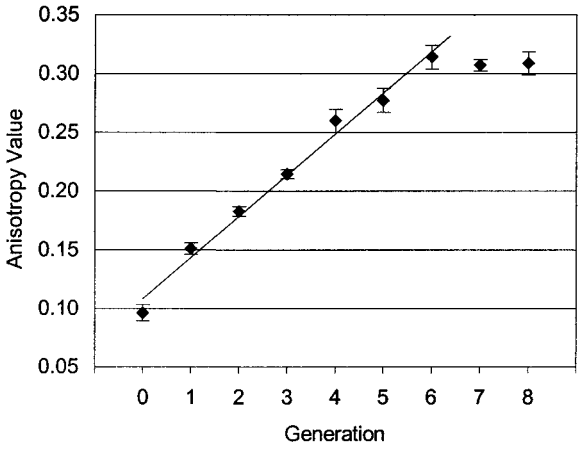


**Figure 5.** Representative steady-state fluorescence anisotropy measurements of phenol blue [$1 \times 10^{-6}$ M] in PAMAM-AT dendrimers [$1 \times 10^{-4}$ M]. The means and standard deviations are shown as error bars for five determinations of the same sample. Standard deviations for all generations are between 0.004 and 0.01. The least squares trend line for G0−6 is shown, $r^2 = 0.988$. Experimental conditions: $\lambda_{ex} = 514$ nm, $\lambda_{em} = 550-600$ nm, and $T = 25$ °C.

**TABLE 2: Representative Fluorescence Lifetimes and Fractional Intensity Contributions Recovered from MEM Analysis**

| medium | $\tau_1$ | $(\alpha_1)^a$ | $\tau_2$ | $(\alpha_2)$ | $\tau_3$ | $(\alpha_3)$ | $\alpha_2/\alpha_3$ |
|---|---|---|---|---|---|---|---|
| water | 0.06 | (0.64) | | | 2.48 | (0.36) | |
| G0[b] | 0.33 | (0.61) | | | 2.13 | (0.29) | |
| G1 | 0.23 | (0.40) | 1.13 | (0.40) | 2.75 | (0.20) | 2.00 |
| G2 | 0.19 | (0.27) | 0.94 | (0.58) | 2.79 | (0.15) | 3.87 |
| G3 | 0.31 | (0.45) | 1.09 | (0.45) | 3.09 | (0.10) | 4.50 |
| G4 | 0.25 | (0.29) | 0.92 | (0.61) | 2.94 | (0.10) | 6.10 |
| G5 | 0.31 | (0.52) | 0.85 | (0.46) | | | |
| G6 | 0.19 | (0.26) | 0.89 | (0.62) | 2.91 | (0.12) | 5.17 |
| G7 | 0.21 | (0.29) | 0.93 | (0.60) | 2.63 | (0.09) | 6.67 |
| G8 | 0.15 | (0.17) | 0.91 | (0.67) | 3.33 | (0.16) | 4.19 |

[a] Results are averages of three replicate measurements of the same sample. Experimental conditions: $\lambda_{ex} = 514$ nm, $\lambda_{em} = 550-600$ nm, kaolin lifetime reference $\tau = 0$ ns, and $T = 25$ °C. [b] An additional short component was resolved at $\tau = 0.01$ ns, $\alpha = 0.10$.

to what was observed for the 560 nm absorption band. No fluorescence spectrum for phenol blue in water could be consistently obtained under these conditions.

Anisotropy values of the phenol blue dendrimer solutions are shown in Figure 5. These values systematically increase from G0 ($0.096 \pm 0.007$) to G6 ($0.31 \pm 0.01$) and then remain constant, within error, for G6−8.

**Fluorescence Lifetimes.** Table 2 shows representative fluorescence lifetimes ($\tau$), fractional intensity contributions ($\alpha$), and $\alpha_2/\alpha_3$ ratios for phenol blue in PAMAM-AT dendrimers recovered by MEM analysis.[64] A representative MEM lifetime distribution is also shown in Figure 6. Three lifetime components were recovered for most samples studied, and they remain relatively constant across dendrimer generations. The shortest-lifetime component, $\tau_1$, is observed in both samples and blanks. Shaver and McGown have documented that this lifetime component is an artifact, and it most frequently occurs with complex decays when utilizing the frequency domain MHF technology and the MEM data analysis software.[65,66] Data analysis indicates the presence of two real lifetime components, which can be attributed to phenol blue. The fractional intensity $\alpha_2$ increases with dendrimer generation at the expense of $\alpha_3$. Though a third discrete lifetime was not resolved for G5 in this particular data set, it is resolved in other data sets and does fit the same trends described here.

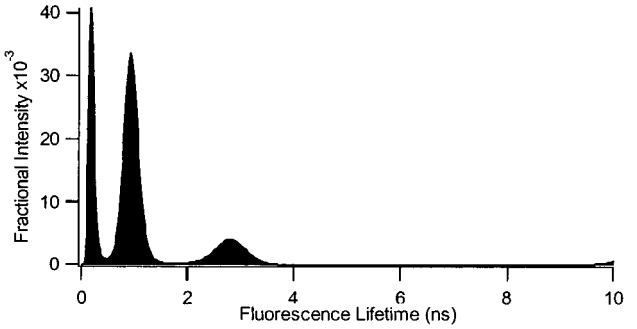


**Figure 6.** Representative MEM plot of the fluorescence lifetime distribution recovered for phenol blue [$1 \times 10^{-6}$ M] in PAMAM-AT G2 [$1 \times 10^{-4}$ M]. Experimental conditions: $\lambda_{ex} = 514$ nm, $\lambda_{em} = 550-600$ nm, kaolin lifetime reference $\tau = 0$ ns, and $T = 25$ °C.

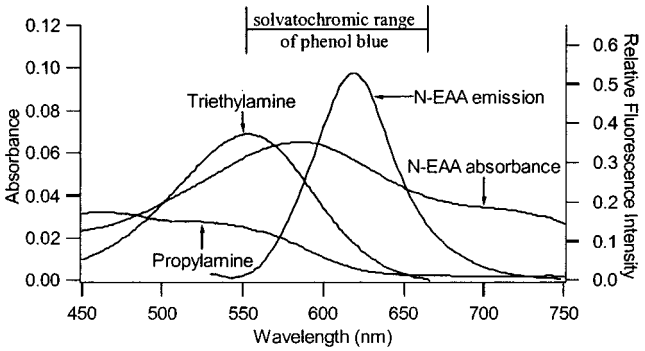


**Figure 7.** Representative absorption and steady-state fluorescence emission spectra of phenol blue [$1 \times 10^{-6}$ M] in neat solutions of selected dendrimer mimic solvents. Experimental conditions: $T = 25$ °C and fluorescence $\lambda_{ex} = 514$ nm.

**Surface and Branching Group Mimics.** Mimics for PAMAM-AT's surface and branching units are examined. *N*-Ethylacetamide (*N*-EAA) is used to mimic the PAMAM-AT dendrimer branching unit. It ($-CH_2-CONH-CH_2-CH_2-$) is one carbon shorter and lacks the amine group of the true branching unit ($-CH_2-CH_2-CONH-CH_2-CH_2-NH_2-$). Propylamine and triethylamine are used to mimic the surface groups and branching points of PAMAM-AT, respectively. While these three compounds do mimic parts of the dendrimer and provide information about the nature of chemical association, they do not mimic the effect of the dendrimer's three-dimensional structure.

Absorption and fluorescence spectra of phenol blue in solutions of these mimics are shown in Figure 7. In general, the spectra have limited similarity to spectra obtained for the dye in dendrimer solutions. In relatively nonpolar triethylamine, phenol blue has a similar absorption $\lambda_{max}$ (553 nm) compared to that in PAMAM-AT ($\lambda_{max}$ 560 nm), but it does not fluoresce. Phenol blue also does not fluoresce in propylamine and absorbs outside of its solvatochromic range, which most likely indicates the formation of a ground-state complex.

In neat *N*-EAA, the absorption and fluorescence emission $\lambda_{max}$ of phenol blue are 584 and 618 nm, respectively. Additional aqueous samples of *N*-EAA were prepared at concentrations of $4 \times 10^{-4}$ and $4 \times 10^{-1}$ M, the same concentrations of the actual branching groups present in $1 \times 10^{-4}$ M solutions of PAMAM-AT G0 and G7, respectively. In the $4 \times 10^{-4}$ concentration *N*-EAA solution, no fluorescence emission of phenol blue is observed, and its absorption spectrum is indistinguishable from that in water. In $4 \times 10^{-1}$ M *N*-EAA, the fluorescence of phenol blue is still not observed, while two partially resolved absorption bands are apparent. The dominant absorption band is not

significantly different from phenol blue in water, and the smaller band is extremely similar to phenol blue in the neat *N*-EAA.

## Discussion

To fully understand and correctly interpret the experimental results, it is important to understand the implications of the dendrimer:dye ratio, which is 100:1. Using Poisson statistics, the probability, $p_i$, of finding $i$ dye molecules in a single dendrimer is

$$p_i = \frac{n^i e^{-n}}{i!}$$

where $n$ is the average number of dye molecules per dendrimer. The probabilities that a single dendrimer contains zero, one, or more than one dye molecule are 0.99005, 0.00990, and 0.00005, respectively. On the basis of these probabilities, the ratio of dendrimers containing a single dye molecule to those containing multiple dye molecules is 198:1. Therefore, the main source of the associated dye's fluorescence can only be attributed to the monomer form of the dye; all other forms (aggregate, excimer, exciplex, etc.) have negligible contribution.

The aforementioned monomer:aggregate probability ratio applies only to dye associated with the dendrimer. It does not apply to the unassociated phenol blue, solvated by water, nor does it mean that the dendrimers have sequestered the majority of the available dye. Aggregation of the aqueous solvated dye is considerably more likely due to the dye's relatively low solubility. The equilibrium between associated and unassociated dye should favor dendrimer association due to the hydrophobicity of phenol blue and the relatively nonpolar interior of PAMAM-AT. The exception would be in the presence of the smallest generations of PAMAM-AT dendrimers, whose solvating abilities are more limited. This notion is supported by the absorption and fluorescence emission spectra, which demonstrate that the larger-generation dendrimers have progressively greater sequestering ability.

Experimental results indicate that the dye definitely associates with the PAMAM-AT dendrimers, and there are clearly two distinct dye populations present. The nature of this dye:dendrimer association is characterized, in part, by studying the dendrimers' surface and branching group mimics. While phenol blue has been shown to fluoresce in the presence of PAMAM-AT dendrimers, the only surface or branching group mimic in which it retains this ability is neat *N*-EAA. Phenol blue's lack of observable steady-state fluorescence in water, propylamine, triethylamine, and aqueous dilutions of *N*-EAA strongly suggests that phenol blue must be associated within the branches of PAMAM-AT dendrimer. The absence of any apparent ground-state complex in absorption data, as seen to occur between phenol blue and the surface group mimic propylamine, also indicates that phenol blue is associated in the PAMAM-AT interior region, beyond where the dye has any interaction with the dendrimer's surface.

This hypothesis as to the location of the dye is further supported by our previous study[40] of PAMAM dendrimers using ET-30. In the present study, the position of the 560 nm absorption band for solutions of phenol blue, in all but the smallest generation dendrimers, is indicative of a nonpolar microenvironment, similar in polarity to furan[50] ($\lambda_{max}$ 562 nm). This is significantly less polar[72] than our previous results with ET-30. We reported that while ET-30 had some interior accessibility, it was not completely encapsulated by the dendrimer. Since both studies were carried out using the same experimental conditions and concentrations, the less polar microenvironment observed with phenol blue must be due to its location further within the dendrimer. The existence and accessibility of such a nonpolar microenvironment within PAMAM-AT dendrimers is rather remarkable considering that they are water-soluble.

The absorption and fluorescence $\lambda_{max}$ values of phenol blue sequestered within PAMAM-AT are indicative of a somewhat less polar microenvironment than is observed for the dye in neat *N*-EAA. However, this can be accounted for by considering that the dye sequestered within PAMAM-AT interior will also interact with the tertiary amine branching points that are shown to be very nonpolar by the mimic triethylamine. All experimental results strongly suggest that the dye population within the PAMAM-AT dendrimer interior is the origin of the absorption band at 560 nm and the predominant source of fluorescence emission. Furthermore, if the majority of the fluorescence emission signal originates from dendrimer associated dye, it is also expected that this dye population will be responsible for the largest fractional intensity recovered in the lifetime distribution ($\tau_2 = 0.9$ ns).

The other absorption band at 646 nm is indicative of a much more polar, predominantly aqueous microenvironment and is considerably less intense in all but the smallest PAMAM-AT generations. As such, very little fluorescence emission is expected from this aqueous dye population. This expectation is confirmed by the trend of increasing relative fluorescence intensity with increasingly larger PAMAM-AT generations. These facts further support the assignment of the second lifetime component, $\tau_2$, as the dendrimer associated dye population. While phenol blue is only weakly fluorescent in water, under lifetime measurement conditions, one real lifetime component ($\tau_3$) is reproducibly recovered. This component is most likely due to an aggregate of the relatively hydrophobic dye molecules in water. The heterogeneity in the third lifetime component ($\tau_3 = 2.78 \pm 0.35$) supports this assumption, since the exact composition of the dye aggregate will vary. The MEM plot in Figure 6 clearly shows that this lifetime component ($\tau_3$) is not discrete but, rather, distributed. Examination of the lifetime distributions for phenol blue in aqueous dendrimer solutions clearly illustrates that the third lifetime component is due to the unassociated dye present in these solutions. The fact that $\tau_2$ is less than $\tau_3$ may seem surprising, but we have discovered that the lifetime of phenol blue is also sensitive to solvent polarity.[73] In neat organic solvents, its lifetime decreases with increasing solvent dielectric constant.[73] It is also important to point out that the fractional intensity contributions, $\alpha_3$, for the unassociated dye decreases with increasing generation. Generation 8 is the exception from this trend and will be discussed in additional detail momentarily. These trends in the lifetime data are keeping with both the absorption and fluorescence emission data.

Although absorption spectra and fluorescence lifetimes clearly show two dye populations in the presence of all but the smallest PAMAM-AT generations, it is not surprising that only one population is apparent in the steady-state fluorescence emission spectra. The dynamic lifetime measurement distinguishes between the two fluorescence signals even when only one is observed in steady-state measurements. In the steady-state mode, one band may obscure another due to its width, close wavelength proximity, and significantly greater intensity. The use of 514 nm as the excitation wavelength may also be a contributing factor; however, the dye's very broad absorption band does encompass this wavelength region.

Fluorescence lifetimes also provide additional microenvironmental information. In general, they are known to lengthen as a fluorophore is sequestered into an increasingly rigid and/or more protected microenvironments such as micelles, cyclodextrins, or dendrimers. However, in our data, there does not appear to be a consistent trend toward longer lifetimes with increasing dendrimer generation for $\tau_2$, the lifetime of dendrimer associated dye. This lifetime data strongly suggests that phenol blue experiences a very similar microenvironment in terms of structural rigidity and accessibility for all generations studied except G0. Examination of the dendrimer structure reveals that only the microcavities near the core would remain unchanged from one generation to the next. Therefore, this may be the specific location of phenol blue within the dendrimer interior.

Increases in the microenvironmental rigidity of the fluorophore are also generally observed as increases in steady-state anisotropy values, since a more rigid/protected microenvironment hinders rotational diffusion. Anisotropy is directly dependent on the rotational correlation time and inversely related to the fluorescence lifetime.[61] Since steady-state anisotropy is a measure of the average rotational motion of the fluorophore increases in the associated dye population and microenvironmental rigidity, both contribute to the observed anisotropy trend (Figure 5). However, these must be minor contributions to the total signal because the fractional intensity ratio of associated with unassociated dye, $\alpha_2$:$\alpha_3$ (Table 2), does not change after G4, and the anisotropy values continue to increase in a systematic, linear fashion. Therefore, the trend in the anisotropy data is best explained by the molecular volume increase seen with dendrimer generation. The statistically indistinguishable anisotropy values ($\sim$ 0.31) for phenol blue associated with G6−8 indicate that the rotational correlation times of dye:dendrimer complex for these larger generations are indistinguishable within the time scale of this measurement. The limiting anisotropy of the probe could not be measured for comparison due to its lack of fluorescence in solvents like glycerol; however, it is expected to be close to the theoretical limit of 0.4.

**Generational Dependencies.** The absorption spectra of phenol blue in G0 shows a small but significant change relative to the aqueous phenol blue solution. The presence of a fluorescence signal from G0 and G1 phenol blue solutions show that they do provide some protection of the dye from water. However, the fluorescence wavelength maxima, $\lambda_{max} = 598$ in G0 and $\lambda_{max} = 582$ in G1, and the relatively low fluorescence intensity indicate that phenol blue's solvational shell still contains water molecules. Given that the anisotropy data shows a relatively "loose" association compared to other generations, only one or perhaps a couple dendrimers are most likely to be associated with a single dye molecule. However, it is clear that extensive dendrimer aggregation around phenol blue does not occur because this would result in a microenvironment that is significantly less polar and more restrictive than what is observed in absorption spectra and anisotropy measurements, respectively. The appearance of the second lifetime component attributed to the G1 associated dye confirms there is an early generational transition from aqueous solvated dye to dendrimer solvated dye.

The largest spectral changes are observed for dye in G2 and G3 PAMAM-AT solutions. The intensity of the 560 nm absorption band and fluorescence emission band increase greatly, while little to no change in the fluorescence $\lambda_{max}$ is observed. These results indicate increasing dye association with these dendrimers and that this association limits the interaction of the dye with water. The increase in the fractional intensity contribution of $\tau_2$ compared to $\tau_3$ in the lifetime distribution for phenol blue in G2 and G3 solutions also confirms this hypothesis.

For phenol blue in G4−7 solutions, comparable absorption and fluorescence emission spectra are recovered, as well as similar fluorescence lifetimes and fractional intensities. This illustrates that these dendrimers are all able to sequester phenol blue, provide a microenvironment of nearly equal polarity, and are kinetically alike over a 48 h period. However, it does appear that G7 provides a marginally less polar microenvironment compared to the other generations, as evident by the fluorescence $\lambda_{max}$. The systematic increase in the fractional intensity contribution belonging to the associated dye ($\alpha_2$), at the expense of the unassociated dye ($\alpha_3$), shows that larger dendrimers enhance the solubility of phenol blue compared to the smaller generations ($\sim$ 30% G1 − G8).

The reverse trends in the data for phenol blue in G8 solutions is consistent with surface group density information found in the literature.[74] There are eight surface groups on PAMAM-AT G1, and this number increases to 1024 surface groups on G8. The experimental data clearly shows that the increased G8 surface density does limit the dye's ability to penetrate the dendrimer surface during the 48 h allowed for equilibration. This fact is observed as decreased fluorescence emission intensity and decreased ratios of both the nonpolar:polar absorption bands and $\alpha_2$:$\alpha_3$ (the lifetime fractional intensity ratio for the associated with unassociated dye).

## Conclusions

The physical properties of the interior regions of PAMAM-AT dendrimers are studied through association with the spectroscopic probe phenol blue. These data clearly show the existence of two different dye populations in the presence of each generation studied except G0. In general, PAMAM-AT dendrimers bind the majority of phenol blue into a tight, rather nonpolar microenvironment. Studies of the surface group mimics clearly show that the majority of the dye does not associate at the dendrimer's surface but, rather, within the PAMAM-AT microcavities, such that phenol blue is completely encapsulated, probably near the EDA core. The second dye population consists of an unassociated self-aggregate and is the result of the dendrimers' inability to sequester 100% of phenol blue during the time frame examined. While longer sample preparation times were studied, sample-aging considerations begin to negate equilibration considerations.

This research effectively groups PAMAM-AT dendrimers G0−8 into three types, which agrees reasonably well with previous reports.[28,39] Generations 0 and 1 have a very open structure and little ability to protect a relatively nonpolar solute from aqueous solvent. Generations 4−8 are all nearly equally capable of solvating a nonpolar solute from water, resulting in similar spectroscopic behavior of phenol blue, which is consistent with the more dense, spheroid-like topologies[39] of the largest generations.[39] Though G4 was identified as having an intermediate oblong shape,[39] G2 and G3 clearly demonstrate intermediate behavior in this study as well. The greatest spectroscopic changes are observed to occur for phenol blue in solutions of these two generations. For this particular probe, it was found that generations 2 and larger all provide microenvironments of nearly equal polarity. Generations up to and including G3 have progressively greater ability to sequester available dye, while larger generations (G4−7) have comparable sequestering abilities for this molecular probe. Somewhat less

dye is associated after 48 h in G8, which is likely due to increased surface group density as this series of dendrimers nears its theoretical limit[74] and agrees with surface packing studies.[39] Since association is still observed, we hypothesized that dye association with G8 is kinetically slow compared to the other generations, and preliminary unpublished data support this hypothesis.

The previously unanswered, fundamental questions regarding the flexibility and rotational freedom inside the dendrimers microcavities have also been addressed here. Systematic increases in anisotropy values are descriptive of both relative increases in the dendrimer associated dye population and increases in molecular volume with increasingly larger generations of PAMAM-AT dendrimers, up to G6. Anisotropy values measured for G6−8 are not statistically different and indicate that there is very little rotational motion in these generations due to their comparatively large molecular volume. The rigidity of the microcavity where phenol blue is sequestered within the PAMAM-AT dendrimers does not appear to be dependent on generation but cannot be completely elucidated due to large contributions to the anisotropy from the dendrimer's increasing molecular volume with generation. The rotational freedom specific to the phenol blue molecule in the microcavity cannot be distinguished from the rotational motion of the dye: dendrimer complex until improved methods of modeling dynamic anisotropy for complex, multiexponential decays are developed.

**Acknowledgment.** The authors would like to thank Spencer J. Flamm for his assistance with some related experiments. This research was supported in part by a grant from the National Science Foundation (CAREER Award Grant No. CHE-9733853) and the University of Missouri∼Columbia Research Council.

## References and Notes

(1) Piotti, M. E.; Rivera, F., Jr.; Bond, R.; Hawker, C. J.; Fréchet, J. M. J. *J. Am. Chem. Soc.* **1999**, *121*, 9471−9472.

(2) Hawker, C. J.; Wooley, K. L.; Fréchet, J. M. *J. Chem. Soc., Perkin Trans. 1* **1993**, *1*, 1287−1297.

(3) Tomalia, D. A.; Berry, V.; Hall, M.; Hedstrand, D. M. *Macromolecules* **1987**, *20*, 1164−1167.

(4) Newkome, G. R.; Moorefield, C. N.; Baker, G. R.; Saunders, M. J.; Grossman, S. H. *Angew. Chem., Int. Ed. Engl.* **1991**, *30*, 1178−1180.

(5) Li, J.; Piehler, L. T.; Qin, D.; Baker, J. R., Jr.; Tomalia, D. A.; Meier, D. J. *Langmuir* **2000**, *16*, 5613−5616.

(6) Tomalia, D. A.; Naylor, A. M.; Goddard, W. A., III. *Angew. Chem., Int. Ed. Engl.* **1990**, *29*, 138−175.

(7) Leon, J. W.; Kawa, M.; Fréchet, J. M. *J. Am. Chem. Soc.* **1996**, *118*, 8847−8859.

(8) Palmer, C. P. *J. Chromatogr. A* **1997**, *780*, 75−92.

(9) Haensler, J.; Szoka, F. C., Jr. *Bioconjugate Chem.* **1993**, *4*, 372−379.

(10) Tang, M.; Redemann, C. T.; Szoka, F. C., Jr. *Bioconjugate Chem.* **1996**, *7*, 703−714.

(11) Ukowska-Latallo, J. F.; Bielinska, A. U.; Johnson, J.; Spindler, R.; Tomalia, D. A.; Baker, J. R. J. *Proc. Natl. Acad. Sci. U.S.A.* **1996**, *1993*, 4897−4902.

(12) Bielinska, A.; Kukowska-Latallo, J.; Johnson, J.; Tomalia, D. A.; Baker, J. R. J. *Nucleic Acids Res.* **1996**, *24*, 2176−2182.

(13) Defoort, J. P.; Nardelli, B.; Huang, W.; Ho, D. D.; Tam, J. P. *Proc. Natl. Acad. Sci. U.S.A.* **1992**, *89*, 3879−3883.

(14) Issberner, J.; Böhme, M.; Grimme, S.; Nieger, M.; Paulus, W.; Vögtle, F. *Tetrahedron: Asymmetry* **1996**, *7*, 2223−2232.

(15) Suh, J.; Hah, S. S.; Lee, S. H. *Bioorg. Chem.* **1997**, *25*, 63−75.

(16) Chow, H.-F.; Mak, C. C. *J. Org. Chem.* **1997**, *62*, 5116−5127.

(17) Bardaji, M.; Caminade, A.-M.; Majoral, J.-P.; Chaudret, B. *Organometallics* **1997**, *16*, 3489−3497.

(18) Martin, V. V.; Ralston, W. H.; Hynes, M. R.; Keana, J. F. W. *Bioconjugate Chem.* **1995**, *6*, 616−623.

(19) Gao, H.; Carlson, J.; Stalcup, A. M.; Heineman, W. R. *J. Chromatogr. Sci* **1998**, *36*, 146−154.

(20) Tanaka, N.; Tanigawa, T.; Hosoya, K.; Kimata, K.; Araki, T.; Terabe, S. *Chem. Lett.* **1992**, 959−962.

(21) Kuzdzal, S. A.; Monnig, C. A.; Newkome, G. R.; Moorefield, C. N. *J. Chem. Soc., Chem. Commun.* **1994**, 2139−2140.

(22) Kuzdzal, S. A.; Monnig, C. A.; Newkome, G. R.; Moorefield, C. N. *J. Am. Chem. Soc.* **1997**, *119*, 2255−2261.

(23) Muijselaar, P. G. H. M.; Claessens, H. A.; Cramers, C. A.; Jansen, J. F. G. A.; Meijer, E. W.; de Brabander-van den Berg, E. M. M.; van der Wal, S. *J. High Resolut. Chrom.* **1995**, *18*, 121−123.

(24) Turro, N. J. *Pure Appl. Chem.* **1995**, *67*, 199−208.

(25) Caminati, G.; Turro, N. J.; Tomalia, D. A. *J. Am. Chem. Soc.* **1990**, *112*, 8515−8522.

(26) ben-Avraham, D.; Schulman, L. S.; Bossmann, S. H.; Turro, C.; Turro, N. J. *J. Phys. Chem. B* **1998**, *102*, 5088−5093.

(27) Gopidas, K. R.; Leheny, A. R.; Caminati, G.; Turro, N. J.; Tomalia, D. A. *J. Am. Chem. Soc.* **1991**, *113*, 7335−7342.

(28) Pistolis, G.; Malliaris, A.; Paleos, C. M.; Tsiourvas, D. *Langmuir* **1997**, *13*, 5870−5875.

(29) Wade, D. A.; Torres, P. A.; Tucker, S. A. *Anal. Chim. Acta* **1999**, *397*, 17−31.

(30) Ottaviani, M. F.; Bossmann, S.; Turro, N. J.; Tomalia, D. A. *J. Am. Chem. Soc.* **1994**, *116*, 661−671.

(31) Ottaviani, M. F.; Turro, C.; Turro, N. J.; Bossmann, S. H.; Tomalia, D. *J. Phys. Chem.* **1996**, *100*, 13667−13674.

(32) Jockusch, S.; Ramirez, J.; Sanghvi, K.; Nociti, R.; Turro, N. J.; Tomalia, D. A. *Macromolecules* **1999**, *32*, 4419−4423.

(33) Turro, C.; Niu, S.; Bossmann, S. H.; Tomalia, D. A.; Turro, N. J. *J. Phys. Chem.* **1995**, *99*, 5512−5517.

(34) Moreno-Bondi, M. C.; Orellana, G.; Turro, N. J. *Macromolecules* **1990**, *23*, 910−912.

(35) Jockusch, S.; Turro, N. J.; Tomalia, D. A. *Macromolecules* **1995**, *28*, 7416−7418.

(36) Ottaviani, M. F.; Turro, N. J.; Jockusch, S.; Tomalia, D. A. *J. Phys. Chem.* **1996**, *100*, 13675−13686.

(37) Drummond, C. J.; Grieser, F.; Healy, T. W. *J. Chem. Soc., Faraday Discuss.* **1986**, *81*, 95−106.

(38) Larson, C. L.; Tucker, S. A. *Appl. Spectrosc.*, **2001**, *55*, 679−683.

(39) Naylor, A. M.; Goddard, W. A., III; Kiefer, G. E.; Tomalia, D. A. *J. Am. Chem. Soc.* **1989**, *111*, 2339−2341.

(40) Richter-Egger, D. L.; Li, H.; Tucker, S. A. *Appl. Spectrosc.* **2000**, *54*, 1151−1156.

(41) Warner, I. M.; McGown, L. B. *Anal. Chem.* **1992**, *64*, 343R-352R.

(42) Agbaria, R. A.; Roberts, E.; Warner, I. M. *J. Phys. Chem.* **1995**, *99*, 10056−10060.

(43) Villegas, M. M.; Neal, S. L. *J. Phys. Chem. A* **1997**, *101*, 6890−6896.

(44) Warner, I. M.; Patonay, G.; Thomas, M. P. *Anal. Chem.* **1985**, *57*, 463A-483A.

(45) McGown, L. B.; Hemmingsen, S. L.; Shaver, J. M.; Geng, L. *Appl. Spectrosc.* **1995**, *49*, 60−66.

(46) Geng, L.; McGown, L. B. *Anal. Chem.* **1992**, *64*, 68−74.

(47) Morley, J. O.; Fitton, A. L. *J. Phys. Chem. A* **1999**, *103*, 11442−11450.

(48) Figueras, J. *J. Am. Chem. Soc.* **1971**, *93*, 3255−3263.

(49) Kolling, O. W. *J. Phys. Chem.* **1991**, *95*, 3950−3954.

(50) Kolling, O. W. *Anal. Chem.* **1981**, *53*, 54−56.

(51) Kolling, O. W.; Goodnight, J. L. *Anal. Chem.* **1973**, *45*, 160−164.

(52) Kolling, O. W.; Goodnight, J. L. *Anal. Chem.* **1974**, *46*, 482−485.

(53) Kolling, O. W. *Anal. Chem.* **1978**, *50*, 212−215.

(54) Ruvinov, S. B.; Yang, X.-J.; Parris, K. D.; Banik, U.; Ahmed, S. A.; Miles, E. W.; Sackett, D. L. *J. Biol. Chem.* **1995**, *270*, 6357−6369.

(55) Sackett, D. L.; Wolff, J. *Anal. Biochem.* **1987**, *167*, 228−234.

(56) Sackett, D. L.; Knutson, J. R.; Wolff, J. *J. Biol. Chem.* **1990**, *265*, 14899−14906.

(57) Daban, J.-R.; Bartolomé, S.; Samsó, M. *Anal. Biochem.* **1991**, *199*, 169−174.

(58) Watkins, D. M.; Sayed-Sweet, Y.; Klimash, J. W.; Turro, N. J.; Tomalia, D. A. *Langmuir* **1997**, *13*, 3136−3141.

(59) Topp, A.; Bauer, B. J.; Tomalia, D. A.; Amis, E. J. *Macromolecules* **1999**, *32*, 7232−7237.

(60) Kessel, D. *Photochem. Photobio.* **1991**, *54*, 481−483.

(61) Lakowicz, J. R. *Principles of Fluorescence Spectroscopy*; Plenum Press: New York, 1983.

(62) Spencer, R. D. Ph.D. Dissertation, University of Illinois, Champaign-Urbana, IL, 1970.

(63) Mitchell, G.; Swift, K. Time-Resolved Laser Spectroscopy in Biochemistry II. *SPIE Proc.* **1990**,*1204*, 270−274.

(64) Brochon, J. C.; Livesey, A. K.; Pouget, J.; Valeur, B. *Chem. Phys. Lett.* **1990**, *174*, 517−522.

(65) Shaver, J. M.; McGown, L. B. *Anal. Chem.* **1996**, *68*, 611−620.
(66) Shaver, J. M.; McGown, L. B. *Anal. Chem.* **1996**, *68*, 9−17.
(67) Neal, S. L. *J. Phys. Chem. A* **1997**, *101*, 6883−6889.
(68) Neal, S. L. *Anal. Chem.* **1997**, *69*, 5109−5120.
(69) Tucker, S. A. Ph.D. Dissertation, University of North Texas: Denton, TX, 1994.
(70) Street, K. W., Jr.; Acree, W. E., Jr. *Analyst* **1986**, *111*, 1197−1201.
(71) Meyerhoffer, S. M.; McGown, L. B. *Anal. Chem.* **1991**, *63*, 2082−2086.
(72) Reichardt, C. *Chem. Rev.* **1994**, *94*, 2319−2358.
(73) Richter-Egger, D. L.; Tucker, S. A. Unpublished results, 2001.
(74) de Gennes, P. G.; Hervet, H. *J. Phys. Lett.* **1983**, *44*, 351−360.